

This discussion paper is/has been under review for the journal Atmospheric Chemistry and Physics (ACP). Please refer to the corresponding final paper in ACP if available.

Atmospheric impacts on climatic variability of surface incident solar radiation

K. Wang¹, R. E. Dickinson², M. Wild³, and S. Liang⁴

¹State Key Laboratory of Earth Surface Processes and Resource Ecology, College of Global Change and Earth System Science, Beijing Normal University, Beijing, 100875, Beijing, China

²Department of Geological Sciences, University of Texas at Austin, Austin, TX 78712, USA

³Institute for Atmospheric and Climate Science, ETH Zürich, 8092 Zürich, Switzerland

⁴Department of Geography, University of Maryland, College Park, MD 20742, USA

Received: 20 April 2012 – Accepted: 23 May 2012 – Published: 6 June 2012

Correspondence to: K. Wang (kcwang@bnu.edu.cn)

Published by Copernicus Publications on behalf of the European Geosciences Union.

14009

Abstract

The Earth's climate system is driven by surface incident solar radiation (R_s). Direct measurements have shown that R_s has undergone significant decadal variations. However, a large fraction of the global land surface is not covered by these observations. Satellite-derived R_s has a good global coverage but is of low accuracy in its depiction of decadal variability. This paper shows that daily to decadal variations of R_s , from both aerosols and cloud properties, can be accurately estimated using globally available measurements of Sunshine Duration (SunDu). In particular, SunDu shows that since the late 1980's R_s has brightened over Europe due to decreases in aerosols but dimmed over China due to their increases. We find that variation of cloud cover controls R_s at a monthly scale but that aerosols determine the variability of R_s at a decadal time scale, in particular, over Europe and China. Because of its global availability and long-term history, SunDu can provide an accurate and continuous proxy record of R_s , filling in values for the blank areas that are not covered by direct measurements. By merging direct measurements collected by global energy budget archive with those derived from SunDu, we obtain a good coverage of R_s over the Northern Hemisphere. From this data, the average increase of R_s from 1982 to 2008 is estimated to be 0.87 W m^{-2} per decade.

1 Introduction

Solar radiation drives the Earth's climate system. The amount that is incident at the surface, denoted R_s , has been shown to undergo significant decadal variations by a surface network of radiometers (Gilgen et al., 1998; Liepert, 2002; Long et al., 2009; Ohmura, 2009; Stanhill and Cohen, 2001; Wild et al., 2005). In particular, direct measurements of limited coverage show that the dimming trend of R_s that occurred up to the late 1980's reversed to a widespread brightening after that (Wild, 2009; Wild et al., 2005). Satellite-derived R_s (Pinker et al., 2005) has a better spatial coverage but may

14010

have spurious variability resulting from changes of satellites, their sensor calibration, and undetected low clouds (Evan et al., 2007). It also can be biased by its exclusion of variations of tropospheric aerosols over land (Wang et al., 2009). Since the observed decadal variation in R_s over Europe (Norris and Wild, 2007) and Asia (Norris and Wild, 2009) is primarily from variation of aerosols, it is not surprising that the decadal variations in satellite-derived R_s have been substantially different from those of radiometer measurements at the surface (Hayasaka et al., 2006; Xia et al., 2006).

This paper improves the surface-based global coverage of estimates of R_s by using Sunshine Duration (SunDu), a measurement initiated 150 yr ago, which records the time during a day that the direct solar beam irradiance exceeds 120 W m^{-2} . It is one of the oldest and most robust measurements related to radiation (Wild, 2009). Worldwide direct R_s measurements only began in the late 1950's. SunDu observations provide a globally-distributed proxy record of R_s at both urban and rural sites with a much higher density than that of the direct measurements as obtained from the of Global Energy Budget Archive (GEBA) (Gilgen et al., 1998). Consequently, these observations allow us to fill in the blank areas of the GEBA coverage.

Several previous studies have established good correlations between SunDu and R_s (Essa and Etman, 2004; Hoyt, 1977; Sanchez et al., 2009; Stanhill and Cohen, 2005). SunDu has been regarded as a measure of cloud cover. However, studies have shown that aerosols can also reduce SunDu (Horseman et al., 2008; Kaiser and Qian, 2002; Raschke et al., 2006; Sanchez-Lorenzo et al., 2008; Sanchez et al., 2009; Tang et al., 2011). This paper further demonstrates that SunDu can be used to estimate R_s globally with sufficient accuracy to establish its year-to-year variations. It then examines the year to decadal variations of R_s and their causes.

14011

2 Data and method

2.1 Sunshine duration data

SunDu records the time during a day that direct solar beam irradiance exceeds 120 W m^{-2} . It was initiated 150 yr ago and is one of the oldest and most robust measurements related to radiation (Wild, 2009). In 1962 the Campbell-Stokes sunshine recorder was recommended as the reference SunDu sensor by the World Meteorological Organization (WMO) to homogenize the data of the worldwide network for SunDu (WMO, 2008).

One advantage of SunDu is that the impact of sensor replacement on SunDu measurement is rather small. Three different types of sunshine duration recorders were used from 1888 to 1987 in the US (Stanhill and Cohen, 2005): first, the Jordan photographic recorder from 1888 to 1907; second, the Maring-Marvin thermometric sunshine recorder from 1893 to the mid-1960s; and third, the Foster photoelectric Sun Switch (beginning in 1953). Replacement of the recording method has been shown to have a negligible effect on the annual SunDu (Stanhill and Cohen, 2005).

The World Meteorological Organization (WMO, 2008) requires that hours of sunshine should be measured with an uncertainty of $\pm 0.1 \text{ h}$ and a resolution of 0.1 h . There has been no standardized method to calibrate SunDu detectors. For outdoor calibration, the pyrheliometric method was recommended as a reference method, which detects the transition of direct solar irradiance through the 120 W m^{-2} threshold (WMO, 2008).

SunDu has been regarded as a measure of cloud cover as direct radiation is generally lower than 80 W m^{-2} for scattered clouds (cumulus, stratocumulus) (WMO, 2008). High and thin cirrus, as well as aerosols only reduce SunDu at low solar elevations, i.e., at times when the incident clear sky solar radiation is not much larger than 120 W m^{-2} .

The National Climate Data Center Integrated Surface Hourly Database (Smith et al., 2011) has approximately 4000 stations that reported SunDu from 1982 to 2008. Data durations of about 2200 of these stations exceed one year, and about 1200 stations have more than ten-year data (Fig. 1). We also used SunDu data obtained from the

14012

The application of the method for estimating R_s from SunDu depends on answers to the following questions: (a) Can SunDu accurately estimate the extent to which aerosols and cloud properties modify R_s spatially and seasonally? (b) Can SunDu provide reliable estimates of interannual and decadal variations of R_s ? The following two sections evaluate these two aspects.

3.2 Seasonal variation of R_s

This analysis indicates that this method accurately predicts seasonal variations in R_s . The seasonal variations are primarily determined by solar zenith angle and cloud variations. The overall standard deviation is 12 W m^{-2} (8.6 % in relative value) with a correlation coefficient of 0.98. Figure 2 shows a comparison between GEBA R_s measurements and those derived from SunDu at one station. Table 1 summarizes the comparisons for all stations.

To further test our method, we calculated monthly anomalies in R_s . For each station, we averaged all available R_s data during the study period from 1982 to 2005 for each month. The monthly anomalies were obtained by removing seasonal cycle from the original monthly R_s data, separately for measured and predicted R_s . Figure 3 illustrates one example of this comparison and all statistical parameters are shown in Table 1, with an overall correlation coefficient of 0.80 averaged from the statistical parameters from each station.

We averaged the anomalies over Europe from all 86 stations, and compared the regional averaged anomalies to the GEBA directly measured values (Fig. 4), and over China from 51 stations (Fig. 5). SunDu-derived R_s also predicts relatively well regional averaged anomalies in R_s and it does a little better over Europe than over China based on regional monthly averages.

14015

3.3 Decadal variation of R_s

Monthly anomaly of R_s depends primarily on variations in cloud cover. However, decadal variation of R_s can also depend strongly on aerosols. We also evaluated how well decadal variations in the SunDu-derived R_s are modeled. Figure 6 shows that the decadal variation in R_s is adequately captured by SunDu-derived R_s in Europe. Figure 7 shows that the SunDu-derived R_s also reasonably predicts the variation before 1990 and after 1993 in China. However, there is a sharp increase in the measured R_s between 1990 and 1993 that is not captured by SunDu. Figure 8 shows that SunDu-derived R_s accurately predicts decadal variation in the baseline stations in China, where the pyranometers used to measure R_s were carefully calibrated and maintained. The discontinuity in the other Chinese data (see Fig. 7) occurs during the period from 1990 to the spring of 1993, when China replaced its Russian-made pyranometers (Type: DFY) with Chinese-made pyranometers (Type: TBS) at most stations (CMA, 1996).

Therefore, it appears that the sharp increase in measured R_s was primarily an artifact of instrument replacement and that SunDu-derived R_s can be used to accurately predict decadal variations of R_s in China. Further evidence for this conclusion is provided by comparison of both estimates of R_s with pan evaporation. Pan evaporation has been shown to be in good agreement with solar radiation (Roderick and Farquhar, 2002). The variation of pan evaporation from the 1980s to the 2000s in China (Cong et al., 2009) is more strongly correlated with SunDu-derived R_s than the directly-measured R_s shown in Fig. 7. The spuriousness of the discontinuity of R_s direct measurements has also been confirmed by quantify-controlled process studies (Tang et al., 2010; Tang et al., 2011). The decrease in SunDu-derived R_s in the period of 1990–1992 results from the abrupt increase in stratospheric aerosols (Stevermer et al., 2000) following the Pinatubo volcano eruption in 1991 and also occurs in the direct measurements.

In summary, after converting SunDu into R_s using the proposed method (Eq. 1), SunDu-derived R_s agrees very well with direct measurements on inter-annual and

14016

only reduce SunDu at low solar elevations. Although, it has been questioned (Stanhill and Cohen, 2005) as to whether SunDu would detect the impact of aerosols on R_s , existing studies have already shown that a reduction in SunDu correlates with increases in atmospheric aerosols (Horseman et al., 2008; Kaiser and Qian, 2002; Qian et al., 2006; Sanchez et al., 2009).

Comparison of Figs. 9 and 11 show that decadal variability of SunDu-derived R_s is dominated by the changes in aerosols, especially those over Europe and China. The Pinatubo volcanic eruption in 1991 produced a large amount of stratospheric aerosols with substantial anomalies in global AOD as seen in Fig. 11 and corresponded to a large reduction in R_s in all regions (Fig. 9). The change of cloud cover in Europe compensated the impact of elevated stratospheric aerosols (Fig. 11a). Except during such eruptions, changes in R_s on the decadal time scale are primarily controlled by tropospheric AOD anomalies, e.g., the brightening over Europe after 1995, during which time Fig. 11a shows increasing cloud cover but decreasing AOD. Direct concurrent measurements of R_s and AOD (Norris and Wild, 2009; Ruckstuhl et al., 2010) have confirmed that the AOD control of R_s , i.e., the solar irradiance increase caused by the direct effect of decreasing aerosol, accounts for most of the observed increase of all-sky solar radiation over Europe from 1981 to 2005.

The decline of R_s since 2000 over China (Fig. 9b) was also a result of increased AOD, since cloud cover decreased at that time (Fig. 11b). The substantial increase of AOD in China from the late 1980s to the early 1990s, was compensated by a reduction in cloud cover (Qian et al., 2006; Warren et al., 2007; Xia, 2012) (Fig. 11b). The dips shown in Figs. 9e and 11e correspond to all the major fires occurring in Indonesia since 1990 (Podgorny et al., 2003; van der Werf et al., 2008), in particular, the 1991, 1994, 1997–1998 fires, and the reported ramp up of burning after 2000 that culminated in the large fires of 2006 (Podgorny et al., 2003; van der Werf et al., 2008).

The connection between R_s and AOD is further clarified by correlating their five-year smoothed monthly anomalies at each station, i.e., the month-to-month variability seen in Fig. 9 was filtered out. Figure 12 shows that about 58 % of all stations with

14019

this smoothing have a correlation coefficient larger than 0.5, indicating that the decadal variation in aerosols contributes more than 25 % of the decadal variance in R_s at the majority of the individual stations. Some sites show low correlation or even negative correlation. At the stations, change of clouds is the determining factor of long-term variation of R_s , such as those in the United States (Long et al., 2009).

4.4 Trend of R_s over the Northern Hemisphere

We have merged measurements of R_s derived by SunDu with those directly measured and collected by GEBA. Monthly anomalies were used to obtain a global trend. Its significance was evaluated using the Mann-Kendall test at each station. About 44 % of the stations passed the 95 % confidence test. Figure 13 shows the long-term trends of R_s as aggregated over $5^\circ \times 5^\circ$ grid boxes (302 boxes). The 252 boxes obtained over the Northern Hemisphere have an average trend of 0.87 W m^{-2} per decade. Only 50 boxes were available for R_s data over the Southern Hemisphere and these have a mean trend of zero.

5 Discussion and conclusions

SunDu has been regarded as primarily an observation of cloud cover and not likely to detect the impact of aerosols on R_s . However, this study shows that SunDu data can describe variations of R_s that are controlled by either cloudiness or aerosols. The SunDu-derived R_s agrees very well with direct measurements on inter-annual and decadal time scales. SunDu as a proxy for R_s provides a stable long-term data series. Compared to its direct measurement, R_s from SunDu appears to be less sensitive to instrument replacement and calibration, and shows that the widely reported sharp increase in R_s during the early 1990s in China was a result of instrument replacement. The surface networks of radiometers (e.g., GEBA) are concentrated in the developed nations of the Northern Hemisphere and in urban areas. SunDu is much more widely available and

14020

provides a long-term time series dataset where direct measurements are not available, such as in South Asia and South America. Thus, estimation of R_s by SunDu is useful as a complement to the globally sparse direct measurements, even in Europe where its direct measurements have the highest density.

5 The estimates of R_s by SunDu are merged with its direct measurements to provide a long global dataset with high spatial coverage over the Northern Hemisphere. This dataset shows an average increase at a rate of 0.87 Wm^{-2} per decade from 1982 to 2008. The average trend over the Southern Hemisphere, whose coverage is much poorer, is negligible. Apparently, the long-term variations of R_s over the two hemispheres are substantially different.

10 The four major datasets used here, SunDu-derived R_s , satellite-measured stratospheric AOD, visibility-derived tropospheric AOD, and visual observations of cloud cover fraction are totally independent. The consistency of their features show that the conventional SunDu observations supply robust information on atmospheric controls of the climate variability of R_s . As such, they would be useful to constrain climate model parameterizations that generate R_s variability. Inter-annual variability of R_s is controlled in most regions by variability of cloud cover and volcanic aerosols, with Indonesia as an exception, where forest fires appear to be the dominant controlling factor. Decadal variability of R_s in most regions especially in Europe, China, and North America (primarily 15 Canada and Mexico), is dominated by variations in tropospheric aerosols. Further analysis would be needed to separate the contributions of direct, indirect, or semi-direct effects of aerosols from the effects of changes in cloud properties. To accomplish this, model simulation is necessary. It needs further study.

25 *Acknowledgements.* The first author was funded by the Global Change Key Research Project (2012CB955302) and National Natural Science Foundation of China (41175126). The second author was funded DOE grant DE-SC0002246, and NSF grant ATM-0720619. The upgrade of the Global Energy Balance Archive has been supported by the Swiss National Competence Center in Climate Research (NCCR climate). The National Climate Data Center Integrated Surface Database (ISD) data were downloaded from ([http://www.ncdc.noaa.gov/oa/climate/isd/](http://www.ncdc.noaa.gov/oa/climate/isd/index.php) 30 index.php).

14021

References

- Angstrom, A.: Solar and terrestrial radiation. Report to the international commission for solar research on actinometric investigations of solar and atmospheric radiation, *Q. J. Roy. Meteor. Soc.*, *50*, 121–126, 1924.
- 5 CMA: Observation method of Meteorological radiation, Meteorological Press, Beijing, 1996.
- Cong, Z. T., Yang, D. W., and Ni, G. H.: Does evaporation paradox exist in China?, *Hydrol. Earth Syst. Sci.*, *13*, 357–366, doi:10.5194/hess-13-357-2009, 2009.
- Dai, A., Karl, T. R., Sun, B., and Trenberth, K. E.: Recent trends in cloudiness over the United States – a tale of monitoring inadequacies, *B. Am. Meteorol. Soc.*, *87*, 597–606, 2006.
- 10 Essa, K. S. and Etman, S. M.: On the relation between cloud cover amount and sunshine duration, *Meteorol. Atmos. Phys.*, *87*, 235–240, 2004.
- Evan, A. T., Heidinger, A. K., and Vimont, D. J.: Arguments against a physical long-term trend in global ISCCP cloud amounts, *Geophys. Res. Lett.*, *34*, L04701, doi:10.1029/2006GL028083, 2004.
- 15 Gilgen, H., Wild, M., and Ohmura, A.: Means and trends of shortwave irradiance at the surface estimated from global energy balance archive data, *J. Climate*, *11*, 2042–2061, 1998.
- Hayasaka, T., Kawamoto, K., Shi, G. Y., and Ohmura, A.: Importance of aerosols in satellite-derived estimates of surface shortwave irradiance over China, *Geophys. Res. Lett.*, *33*, L06802, doi:10.1029/2005GL025093, 2006.
- 20 Hess, M., Koepke, P., and Schult, I.: Optical properties of aerosols and clouds: the software package OPAC, *B. Am. Meteorol. Soc.*, *79*, 831–844, 1998.
- Holben, B. N., Eck, T. F., Slutsker, I., Tanré, D., Buis, J. P., Setzer, A., Vermote, E., Reagan, J. A., Kaufman, Y. J., Nakajima, T., Lavenu, F., Jankowiak, I., and Smirnov, A.: AERONET – a federated instrument network and data archive for aerosol characterization, *Remote Sens. Environ.*, *66*, 1–16, 1998.
- 25 Horseman, A., MacKenzie, A. R., and Timmis, R.: Using bright sunshine at low-elevation angles to compile an historical record of the effect of aerosol on incoming solar radiation, *Atmos. Environ.*, *42*, 7600–7610, 2008.
- Hoyt, D. V.: Percent of possible sunshine and the total cloud cover, *Mon. Weather Rev.*, *105*, 648–652, 1977.
- 30

14022

- Kaiser, D. P. and Qian, Y.: Decreasing trends in sunshine duration over China for 1954–1998: indication of increased haze pollution?, *Geophys. Res. Lett.*, 29, 2042, doi:10.1029/2002GL016057, 2002.
- Liang, F. and Xia, X. A.: Long-term trends in solar radiation and the associated climatic factors over China for 1961–2000, *Ann. Geophys.*, 23, 2425–2432, doi:10.5194/angeo-23-2425-2005, 2005.
- Liepert, B. G.: Observed reductions of surface solar radiation at sites in the United States and worldwide from 1961 to 1990, *Geophys. Res. Lett.*, 29, 1421, doi:10.1029/2002GL014910, 2002.
- 10 Long, C. N., Dutton, E. G., Augustine, J. A., Wiscombe, W., Wild, M., McFarlane, S. A., and Flynn, C. J.: Significant decadal brightening of downwelling shortwave in the continental United States, *J. Geophys. Res.*, 114, D00D06, doi:10.1029/2008JD011263, 2009.
- Norris, J. R. and Wild, M.: Trends in aerosol radiative effects over Europe inferred from observed cloud cover, solar “dimming” and solar “brightening”, *J. Geophys. Res.*, 112, D08214, doi:10.1029/2006JD007794, 2007.
- 15 Norris, J. R. and Wild, M.: Trends in aerosol radiative effects over China and Japan inferred from observed cloud cover, solar “dimming” and solar “brightening”, *J. Geophys. Res.*, 114, D00D15, doi:10.1029/2008JD011378, 2009.
- Ohmura, A.: Observed decadal variations in surface solar radiation and their causes, *J. Geophys. Res.*, 114, D00D05, doi:10.1029/2008JD011290, 2009.
- 20 Pinker, R. T., Zhang, B., and Dutton, E. G.: Do satellites detect trends in surface solar radiation?, *Science*, 308, 850–854, 2005.
- Podgorny, I. A., Li, F., and Ramanathan, V.: Large aerosol radiative forcing due to the 1997 Indonesian forest fire, *Geophys. Res. Lett.*, 30, 1028, doi:10.1029/2002GL015979, 2003.
- 25 Prescott, J. A.: Evaporation from water surface in relation to solar radiation, *T. Roy. Soc. South Aust.*, 64, 114–118, 1940.
- Qian, Y., Kaiser, D. P., Leung, L. R., and Xu, M.: More frequent cloud-free sky and less surface solar radiation in China from 1955 to 2000, *Geophys. Res. Lett.*, 33, L01812, doi:10.1029/2005GL024586, 2006.
- 30 Raschke, E., Bakan, S., and Kinne, S.: An assessment of radiation budget data provided by the ISCCP and GEWEX-SRB, *Geophys. Res. Lett.*, 33, L07812, doi:10.1029/2005GL025503, 2006.

14023

- Roderick, M. L. and Farquhar, G. D.: The cause of decreased pan evaporation over the past 50 years, *Science*, 298, 1410–1411, 2002.
- Ruckstuhl, C., Norris, J. R., and Philipona, R.: Is there evidence for an aerosol indirect effect during the recent aerosol optical depth decline in Europe?, *J. Geophys. Res.*, 115, D04204, doi:10.1029/2009JD012867, 2010.
- 5 Sanchez-Lorenzo, A., Calbo, J. and Martin-Vide, J.: Spatial and temporal trends in sunshine duration over Western Europe (1938–2004), *J. Climate*, 21, 6089–6098, 2008.
- Sanchez-Lorenzo, A., Calb, J., Brunetti, M., and Deser, C.: Dimming/brightening over the Iberian Peninsula: trends in sunshine duration and cloud cover and their relations with atmospheric circulation, *J. Geophys. Res.*, 114, D00D09, doi:10.1029/2008JD011394, 2009.
- 10 Shi, G. Y., Hayasaka, T., Ohmura, A., Chen, Z. H., Wang, B., Zhao, J. Q., Che, H. Z., and Xu, L.: Data quality assessment and the long-term trend of ground solar radiation in China, *J. Appl. Meteorol. Clim.*, 47, 1006–1016, 2008.
- Smith, A., Lott, N., and Vose, R.: The integrated surface database recent developments and partnerships, *B. Am. Meteorol. Soc.*, 92, 704–708, 2011.
- 15 Stanhill, G. and Cohen, S.: Global dimming: a review of the evidence for a widespread and significant reduction in global radiation with discussion of its probable causes and possible agricultural consequences, *Agr. Forest Meteorol.*, 107, 255–278, 2001.
- Stanhill, G. and Cohen, S.: Solar radiation changes in the United States during the twentieth century: evidence from sunshine measurements, *J. Climate*, 18, 1503–1512, 2005.
- 20 Stevermer, A. J., Petropavlovskikh, I. V., Rosen, J. M., and DeLuisi, J. J.: Development of a global stratospheric aerosol climatology: optical properties and applications for UV, *J. Geophys. Res.*, 105, 22763–22776, 2000.
- Tang, W.-J., Yang, K., He, J., and Qin, J.: Quality control and estimation of global solar radiation in China, *Sol. Energy*, 84, 466–475, 2010.
- 25 Tang, W.-J., Yang, K., Qin, J., Cheng, C. C. K., and He, J.: Solar radiation trend across China in recent decades: a revisit with quality-controlled data, *Atmos. Chem. Phys.*, 11, 393–406, doi:10.5194/acp-11-393-2011, 2011.
- Wang, K., Dickinson, R. E., and Liang, S.: Clear sky visibility has decreased over land globally from 1973 to 2007, *Science*, 323, 1468–1470, 2009.
- 30 Warren, S. G., Eastman, R. M., and Hahn, C. J.: A survey of changes in cloud cover and cloud types over land from surface observations, 1971–96, *J. Climate*, 20, 717–738, 2007.

14024

- van der Werf, G. R., Dempewolf, J., Trigg, S. N., Randerson, J. T., Kasibhatla, P. S., Gigliof, L., Murdiyarso, D., Peters, W., Morton, D. C., Collatz, G. J., Dolman, A. J., and DeFries, R. S.: Climate regulation of fire emissions and deforestation in equatorial Asia, *P. Natl. Acad. Sci. USA*, 105, 20350–20355, 2008.
- 5 Wielicki, B. A., Wong, T. M., Allan, R. P., Slingo, A., Kiehl, J. T., Soden, B. J., Gordon, C. T., Miller, A. J., Yang, S. K., Randall, D. A., Robertson, F., Susskind, J., and Jacobowitz, H.: Evidence for large decadal variability in the tropical mean radiative energy budget, *Science*, 295, 841–844, 2002.
- Wild, M.: Global dimming and brightening: a review, *J. Geophys. Res.*, 114, D00D16, doi:10.1029/2008JD011470, 2009.
- 10 Wild, M., Gilgen, H., Roesch, A., Ohmura, A., Long, C. N., Dutton, E. G., Forgan, B., Kallis, A., Russak, V., and Tsvetkov, A.: From dimming to brightening: decadal changes in solar radiation at Earth's surface, *Science*, 308, 847–850, 2005.
- Wild, M., Trüssel, B., Ohmura, A., Long, C. N., König-Langlo, G., Dutton, E. G., and Tsvetkov, A.: Global dimming and brightening: an update beyond 2000, *J. Geophys. Res.*, 114, D00D13, doi:10.1029/2008JD011382, 2009.
- 15 WMO: Measurement of sunshine duration, WMO guide to meteorological instruments and methods of observation manual on the global observing system, WMO, <http://www.wmo.int/pages/prog/www/IMOP/publications/CIMO-Guide/CIMO%20Guide%207th%20Edition,%202008/Part%20I/Chapter%208.pdf> (last access: June 2012), 2008.
- 20 Xia, X.: A closer looking at dimming and brightening in China during 1961–2005, *Ann. Geophys.*, 28, 1121–1132, doi:10.5194/angeo-28-1121-2010, 2010.
- Xia, X.: Significant decreasing cloud cover during 1954–2005 due to more clear-sky days and less overcast days in China and its relation to aerosol, *Ann. Geophys.*, 30, 573–582, doi:10.5194/angeo-30-573-2012, 2012.
- 25 Xia, X. A., Wang, P. C., Chen, H. B., and Liang, F.: Analysis of downwelling surface solar radiation in China from National Centers for Environmental Prediction reanalysis, satellite estimates, and surface observations, *J. Geophys. Res.*, 111, D09103, doi:10.1029/2005JD006405, 2006.
- 30 Yang, K., Koike, T., and Ye, B. S.: Improving estimation of hourly, daily, and monthly solar radiation by importing global data sets, *Agr. Forest Meteorol.*, 137, 43–55, 2006.

14025

Table 1. A summary of the locations of the 137 stations in Europe and China where GEBA R_s measurements and estimates from SunDu and AOD overlap for at least 84 months. The statistical parameters of the comparison between R_s measurements and estimates are shown. To show the capability of the method to quantify the effect of clouds on R_s , the statistical parameters of the comparisons of predicted and measured monthly R_s anomalies are also shown as standard deviation (STD), bias and averaged R_s in Wm^{-2} .

Station No.	Station Name	Country	Lat (°)	Lon (°)	Monthly R_s			Monthly R_s anomaly		Averaged R_s
					STD	Bias	R	STD	R	
1169	Innsbruck Univ.	AUSTRIA	47.27	11.40	14.3	-11.6	0.97	13.4	0.64	128.9
1182	Sofia	BULGARIA	42.68	23.33	20.3	15.5	0.97	17.9	0.58	136.8
1188	Locarno-Monti	SWITZERLAND	46.17	8.78	13.0	-13.2	0.99	11.0	0.82	147.2
1189	Hradec Kralove	CZECH REPUBLIC	50.25	15.85	12.6	-15	0.99	8.7	0.86	120.7
1190	Ostrava-Poruba	CZECH REPUBLIC	49.82	18.15	15.2	-8.5	0.98	12.8	0.60	112.2
1191	Strbske Pleso	SLOVAKIA	49.12	20.08	12.8	-9.5	0.98	11.2	0.74	122.0
1192	Churanov	CZECH REPUBLIC	49.07	13.62	11.5	-8.4	0.99	11.1	0.76	122.1
1193	Kucharovice	CZECH REPUBLIC	48.88	16.08	8.6	-3.0	1.00	6.4	0.91	126.6
1195	Bratislava	SLOVAKIA	48.17	17.10	11.1	-11.9	0.99	8.2	0.82	134.9
1197	Potsdam	GERMANY	52.38	13.10	5.9	-1.4	1.00	5.4	0.96	114.3
1199	Fichtelberg	GERMANY	50.43	12.95	23.0	-4.5	0.95	19.3	0.58	110.3
1202	Norderney	GERMANY	53.72	7.15	10.6	-11.9	1.00	6.7	0.93	117.6
1203	Hamburg	GERMANY	53.65	10.12	6.5	0.8	1.00	6.0	0.96	106.3
1204	Bremen	GERMANY	53.05	8.80	7.5	-4.7	0.99	7.2	0.90	107.0
1205	Braunschweig	GERMANY	52.30	10.45	5.6	-5.1	1.00	4.9	0.97	115.0
1206	Osnabrueck	GERMANY	52.25	8.05	5.5	-5.5	1.00	5.0	0.97	112.0
1207	Bocholt	GERMANY	51.83	6.53	6.4	-7.0	1.00	5.9	0.95	116.8
1208	Bad Lippspringe	GERMANY	51.78	8.83	6.8	-4.2	1.00	6.3	0.95	109.3
1209	Braunlage	GERMANY	51.72	10.62	8.0	-2.4	0.99	7.5	0.92	110.3
1210	Gelsenkirchen	GERMANY	51.50	7.08	6.0	0.1	1.00	5.7	0.94	108.3
1211	Kassel	GERMANY	51.30	9.45	6.3	-6.0	1.00	5.7	0.95	113.5
1212	Bonn	GERMANY	50.70	7.15	7.4	-4.9	0.99	7.3	0.91	113.3
1213	Giessen	GERMANY	50.58	8.70	8.0	-5.3	0.99	7.6	0.93	116.0
1214	Coburg	GERMANY	50.27	10.95	8.8	-6.8	0.99	8.0	0.92	119.2
1216	Wuerzburg	GERMANY	49.77	9.97	8.4	-13.2	1.00	5.9	0.95	125.3
1217	Trier	GERMANY	49.75	6.67	9.9	-8.3	1.00	7.6	0.93	121.3
1218	Mannheim	GERMANY	49.52	8.55	6.6	-4.3	1.00	6.2	0.95	121.3
1219	Nuernberg	GERMANY	49.5	11.08	6.4	-3.8	1.00	6.1	0.96	119.5

14026

Table 1. Continued.

Station No.	Station Name	Country	Lat (°)	Lon (°)	Monthly R_s			Monthly R_s anomaly		Averaged R_s
					STD	Bias	R	STD	R	
1220	Saarbruecken	GERMANY	49.22	7.12	9.2	-5.4	0.99	8.7	0.93	119.1
1221	Weissenburg	GERMANY	49.02	10.97	7.1	-6.7	1.00	6.7	0.91	124.5
1223	Passau	GERMANY	48.58	13.47	6.7	-9.3	1.00	5.6	0.94	126.7
1224	Weihenstephan	GERMANY	48.40	11.70	9.3	-11.0	0.99	7.3	0.88	126.6
1225	Freiburg	GERMANY	48.00	7.85	17.9	-1.0	0.98	13.2	0.72	129.1
1226	Hohenpeissenberg	GERMANY	47.80	11.02	9.6	-16.1	0.99	8.6	0.87	135.4
1228	Santander	SPAIN	43.47	-3.82	9.8	-6.2	0.99	8.7	0.82	142.1
1229	Oviedo	SPAIN	43.35	-5.87	8.9	-1.5	0.99	8.2	0.85	135.7
1230	Piikkio	FINLAND	42.47	-2.40	10.7	-9.4	0.99	9.5	0.77	160.7
1231	Madrid-Universitaet	EL SALVADOR	40.45	-3.72	10.1	-8.3	0.99	8.5	0.81	188.9
1233	Palma de Mallorca	SPAIN	39.55	2.62	10.0	-9.0	0.99	8.1	0.72	181.1
1234	Caceres	SPAIN	39.47	-6.33	9.0	-7.3	0.99	7.4	0.90	195.2
1241	Reims	FRANCE	49.30	4.03	19.9	-21.4	0.97	17.3	0.53	129.9
1242	Caen	FRANCE	49.18	-0.47	20.3	-15.8	0.96	19.1	0.46	129.1
1243	Paris-Montsouris	FRANCE	48.82	2.33	13.7	1.8	0.98	12.7	0.7	109.5
1245	Trappes	FRANCE	48.77	2.02	14.7	-11.9	0.98	12.8	0.66	124.9
1246	Nancy-Essey	FRANCE	48.68	6.22	9.1	-12.2	1.00	7.2	0.92	125.9
1247	Strassburg	FRANCE	48.55	7.63	10.9	-12.9	0.99	8.6	0.86	129.0
1248	Rennes	FRANCE	48.07	-1.73	8.1	-8.8	0.99	7.3	0.89	129.9
1249	Auxerre	FRANCE	47.80	3.55	12.7	-13.8	0.99	8.7	0.84	125.3
1257	Limoges	FRANCE	45.82	1.28	10.1	-6.5	0.99	9.0	0.88	144.5
1258	Clermont-Ferrand	FRANCE	45.78	3.17	8.4	-9.8	0.99	7.7	0.87	144.4
1259	Bordeaux	FRANCE	44.83	-0.70	6.9	-6.8	1.00	6.2	0.91	149.9
1261	Biscarrosse	FRANCE	44.43	-1.25	9.3	-6.7	0.99	8.1	0.84	151.8
1264	Millau	FRANCE	44.12	3.02	25.3	-18.6	0.95	24	0.58	159.4
1266	Nice	FRANCE	43.65	7.20	9.8	-11.8	0.99	7.8	0.81	175.3
1268	Marignane	FRANCE	43.43	5.22	6.0	-10.0	1.00	4.9	0.91	176.7
1274	Ajaccio	FRANCE	41.92	8.80	9.3	-11.0	0.99	8.1	0.77	182.5
1320	Budapest	HUNGARY	47.43	19.18	13.5	-15.3	0.99	11.6	0.65	136.2
1324	Szarvas	HUNGARY	46.87	20.53	17.3	-29.5	0.98	13.8	0.55	146.2
1329	Malin Head,C.	IRELAND	55.37	-7.33	8.0	-10.3	1.00	5.6	0.88	106.7
1331	Clones	IRELAND	54.18	-7.23	9.0	-7.0	0.99	8.4	0.77	102.3
1332	Dublin Airport	IRELAND	53.43	-6.25	7.9	-7.6	0.99	7.5	0.81	110.4
1333	Birr	IRELAND	53.08	-7.88	8.6	-9.2	0.99	8.0	0.80	111.5
1334	Kilkenny	IRELAND	52.67	-7.27	8.4	-9.3	0.99	7.4	0.84	114.2
1379	Eelde	NETHERLANDS	53.13	6.58	8.5	-9.2	0.99	7.6	0.92	109.0

14027

Table 1. Continued.

Station No.	Station Name	Country	Lat (°)	Lon (°)	Monthly R_s			Monthly R_s anomaly		Averaged R_s
					STD	Bias	R	STD	R	
1380	De Kooy	NETHERLANDS	52.92	4.78	15.7	-14.6	0.99	12	0.82	121.2
1381	De Bilt	NETHERLANDS	52.10	5.18	8.8	-7.7	0.99	7.9	0.90	111.1
1382	Vlissingen	NETHERLANDS	51.45	3.60	9.4	-14.3	1.00	6.6	0.92	122.8
1383	Beek/Limburg	NETHERLANDS	50.92	5.77	8.1	-8.6	0.99	7.3	0.92	119.0
1393	Zakopane	POLAND	49.28	19.97	15.8	0.0	0.97	13.0	0.61	113.2
1481	Praha/(Prag-Karlovy)	CZECH REPUBLIC	50.07	14.43	8.1	-3.7	0.99	7.8	0.85	114.2
1572	Zuerich-Kloten	SWITZERLAND	47.48	8.53	8.1	-10.2	0.99	7.1	0.91	125.8
2040	Urumqi	CHINA	43.78	87.62	12.3	5.7	0.99	9.3	0.73	161.1
2042	Beijing	CHINA	39.93	116.28	10.0	8.8	0.99	7.4	0.87	157.9
2043	Lanzhou	CHINA	36.05	103.88	10.9	21.3	0.99	8.8	0.8	160.9
2044	Shanghai	CHINA	31.4	121.48	14.9	12.6	0.94	13.8	0.78	145.7
2045	Chengdu	CHINA	30.67	104.02	9.9	26.7	0.98	8.4	0.84	103.9
2047	Kunming	CHINA	25.02	102.68	15.2	9.2	0.93	12.4	0.87	175.2
2048	Guangzhou	CHINA	23.13	113.32	16.9	27.1	0.89	12.6	0.80	127.6
2077	Bastia	FRANCE	42.55	9.48	8.1	-10.3	0.99	7.1	0.83	175.2
2108	Saentis	SWITZERLAND	47.25	9.35	17.9	-37	0.96	14.5	0.62	149.7
2109	Payerne SMA	SWITZERLAND	46.82	6.95	7.2	-9.1	1.00	5.6	0.93	134.2
2110	Payerne BSRN	SWITZERLAND	46.82	6.95	11.3	-18.4	1.00	6.4	0.91	137.9
2111	Davos	SWITZERLAND	46.8	9.82	17.1	-30.4	0.97	11.4	0.67	153.1
2112	La Dole	SWITZERLAND	46.43	6.10	20.1	-4.4	0.98	11.6	0.81	133.6
2113	Geneve	SWITZERLAND	46.25	6.13	8.7	-9.1	1.00	7.1	0.90	140.2
2114	Basel	SWITZERLAND	47.55	7.58	11.7	-9.8	0.99	11.1	0.78	130.0
2133	Brest	FRANCE	48.45	-4.42	10.9	-8.1	0.99	10.0	0.84	128.0
2134	Bourges	FRANCE	47.07	2.37	9.6	-13.4	0.99	7.2	0.90	141.4
2471	Marseille/Marignane	FRANCE	43.45	5.23	10.6	-11.0	0.99	9.0	0.78	183.2
2472	Montlimar	FRANCE	44.58	4.73	9.0	-10.0	0.99	6.9	0.87	165.9
2734	Golmud	CHINA	36.42	94.90	9.5	1.0	0.99	8.6	0.80	220.4
2739	Shantou	CHINA	23.40	116.68	13.4	17.5	0.95	11.0	0.87	157.2
2740	Nanning	CHINA	22.82	108.35	19.2	13.3	0.93	16.6	0.76	144.5
2741	Haikou	CHINA	20.03	110.35	20.1	23.3	0.92	18.5	0.71	154.6
2742	Fuzhou	CHINA	26.08	119.28	19.3	14.8	0.92	16.8	0.73	138.1
2744	Nanjing	CHINA	32.00	118.80	11.6	22.8	0.97	9.5	0.88	137.1
2745	Hefei	CHINA	31.87	117.23	18.3	21.9	0.92	16.9	0.70	136.2
2746	Chongqing	CHINA	29.58	106.47	9.9	27.0	0.98	8.5	0.89	99.3
2747	Changsha	CHINA	28.22	112.92	15.8	21.5	0.96	12.9	0.82	126.7
2748	Guiyang	CHINA	26.58	106.72	16.4	24.4	0.93	15.3	0.71	111.3

14028

Table 1. Continued.

Station No.	Station Name	Country	Lat (°)	Lon (°)	Monthly R_s			Monthly R_s anomaly		Averaged R_s
					STD	Bias	R	STD	R	
2749	Guilin	CHINA	25.32	110.30	21.3	29.4	0.9	18.5	0.62	123.0
2750	Jinghong	CHINA	22.00	100.80	19.9	7.6	0.85	16.1	0.59	177.4
2751	Xi'an	CHINA	34.30	108.93	16.6	5.8	0.96	15.6	0.72	135.0
2752	Jinan	CHINA	36.68	116.98	15.7	21.8	0.96	14.0	0.65	149.1
2753	Erlanhaote	CHINA	43.65	111.97	11.6	-10.9	0.99	9.7	0.55	198.0
2754	Yinchuan	CHINA	38.48	106.22	10.3	-3.3	0.99	8.4	0.81	189.9
2755	Taiyuan	CHINA	37.78	112.55	12.3	8.2	0.98	9.8	0.77	160.6
2756	Changchun	CHINA	43.90	125.22	14.4	-3.0	0.97	13.7	0.55	158.7
2757	Tianjin	CHINA	39.08	117.07	17.4	7.8	0.95	17.0	0.61	155.0
2759	Hami	CHINA	42.82	93.52	10.6	-6.3	0.99	6.9	0.78	196.5
2760	Xining	CHINA	36.62	101.77	19.2	18.8	0.94	17.8	0.53	172.1
2761	Heihe	CHINA	50.25	127.45	11.1	1.9	0.99	10.1	0.8	141.8
2769	Altay	CHINA	47.73	88.08	15.0	0.1	0.99	9.3	0.78	172.4
2771	Dunhuang	CHINA	40.15	94.68	13.4	-2.0	0.99	11.0	0.66	202.6
2774	Nanchang	CHINA	28.60	115.92	15.7	22.9	0.95	11.5	0.85	135.1
2776	Hailaer	CHINA	49.22	119.75	11.1	-2.8	0.99	9.5	0.65	157.2
2780	Luzhou	CHINA	28.83	105.43	11.1	29.3	0.98	9.8	0.86	105.9
2781	Tengchong	CHINA	25.02	98.50	18.1	5.5	0.83	13.8	0.80	172.6
2782	Mianyang	CHINA	31.47	104.68	9.5	16.7	0.98	8.6	0.84	113.6
2787	Datong	CHINA	40.1	113.33	14.3	0.3	0.98	13.3	0.54	171.0
2790	Minqin	CHINA	38.63	103.08	14.5	5.4	0.98	10.6	0.70	195.1
2791	Ganzhou	CHINA	25.85	114.95	14.3	19.1	0.96	10.8	0.85	141.1
2792	Turpan	CHINA	42.93	89.20	13.8	3.5	0.99	11.5	0.55	173.5
2801	Yan'an	CHINA	36.60	109.50	12.1	17.9	0.98	10.6	0.82	157.7
2803	Xilinhaote	CHINA	43.95	116.07	11.5	3.7	0.99	8.7	0.74	174.6
2805	Yanji	CHINA	42.83	129.47	15.5	-2.3	0.96	13.0	0.68	146.8
2806	Chaoyang	CHINA	41.55	120.45	10.6	2.7	0.98	9.8	0.67	167.5
2812	Lijiang	CHINA	26.87	100.22	15.1	6.8	0.90	14.0	0.77	193.8
2813	Mengzi	CHINA	23.38	103.38	15.9	10.0	0.90	13.8	0.73	176.0
2838	Weining	CHINA	26.85	104.25	15.6	23.7	0.92	12.0	0.87	149.8
2843	Shanghai(1961–1990)	CHINA	31.17	121.43	14.3	18.7	0.95	11.6	0.84	139.0
2845	Shaoguan	CHINA	24.80	113.60	18.9	35.3	0.93	14.3	0.73	124.3
2846	Zunyi	CHINA	27.68	106.92	12.3	34.4	0.98	8.1	0.89	98.2
2852	Zhaotong	CHINA	27.33	103.75	14.1	8.6	0.96	13.6	0.85	163.2
2867	Wageningen	NETHERLANDS	51.97	5.65	10.0	-4.6	0.99	9.7	0.86	108.1
Average					12.0	-1.0	0.98	10.1	0.80	140.0

14029

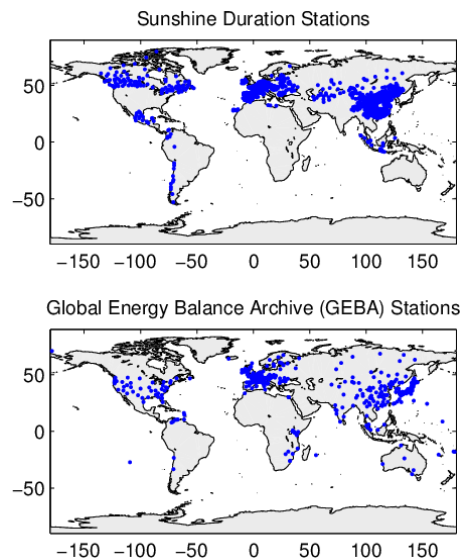


Fig. 1. A map of the Global Energy Balance Archive (GEBA) and Sunshine Duration (SunDu) stations. SunDu data are from the National Climate Data Center (NCDC) Integrated Surface Hourly Database and Chinese SunDu data are obtained from the Chinese Meteorological Administration. Each point in upper pannel represents a SunDu station where more than 120 months of data of SunDu are available (1165 stations in total). Considering the data availability, we divided the stations into six geographic regions: Europe (35° N–65° N, 10° W–40° E), Iran (20° N–50° N, 30° E–55° E), Indonesia (20° S–20° N, 65° E–130° E), China (20° N–55° N, 55° E–150° E), North America (primarily Canada and Mexico, 15° N–65° N, 160° W–60° W), and Chile (60° S–15° N, 90° W–35° W). The number of stations in the regions are 373 (Europe), 26 (Iran), 417 (China), 75 (Indonesia), 119 (Canada and Mexico), and 26 (Chile).

14030

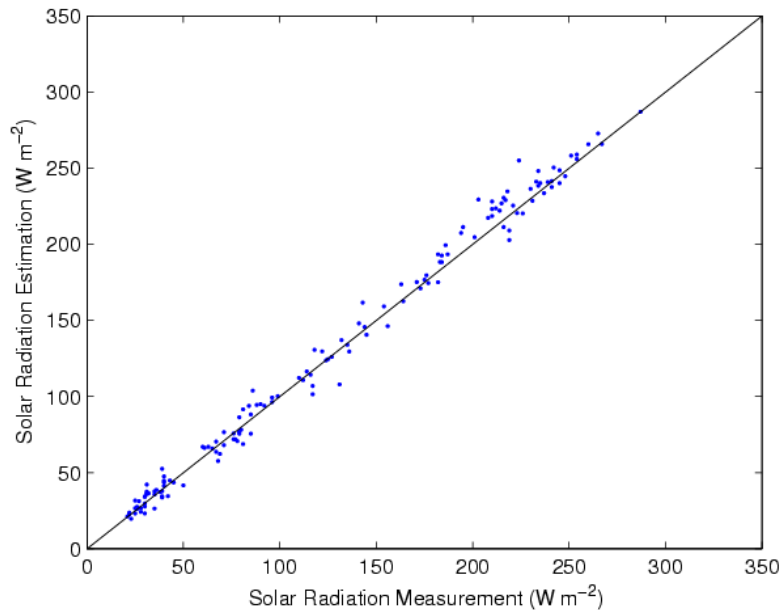


Fig. 2. An example of the comparison between monthly averages of solar radiation (R_s) measurements and our prediction from SunDu at GEBA station No. 1193 (Kucharovice, CZECH REPUBLIC, see Table 1). More information on other stations is available in Table 1.

14031

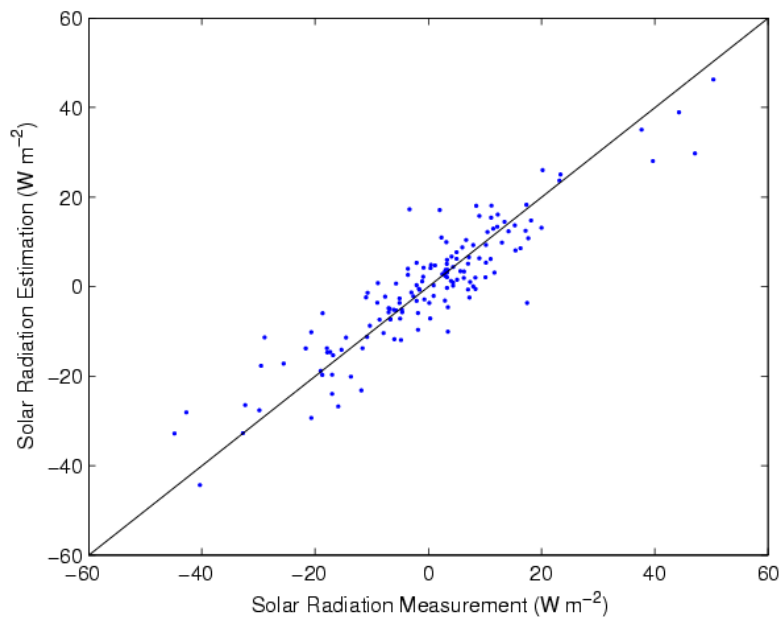


Fig. 3. An example of the comparison between monthly R_s anomalies from direct measurements and our prediction from SunDu at GEBA station No. 1193 (Kucharovice, see Table 1). More information on other stations is available in Table 1.

14032

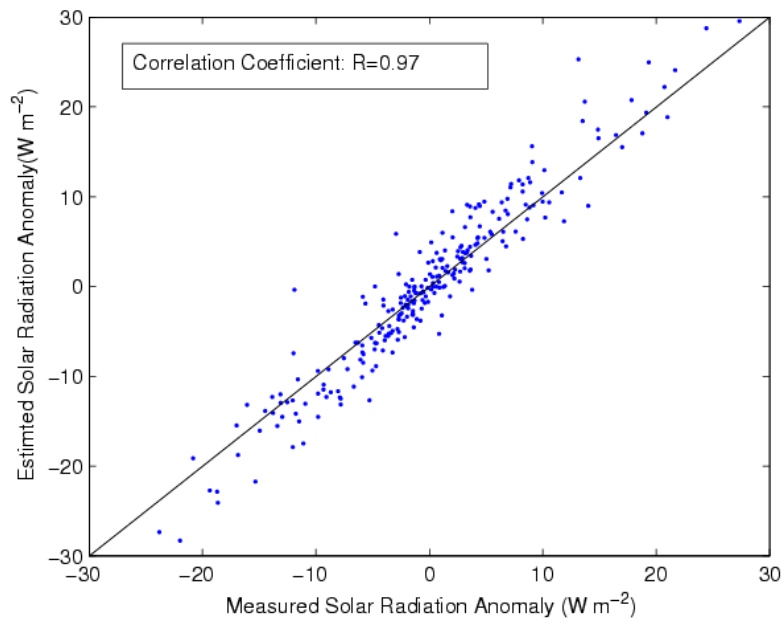


Fig. 4. Comparison between monthly regional R_s anomalies of measurements and our prediction from SunDu. The regional average is over 86 stations in Europe (Table 1). Each point represents one month.

14033

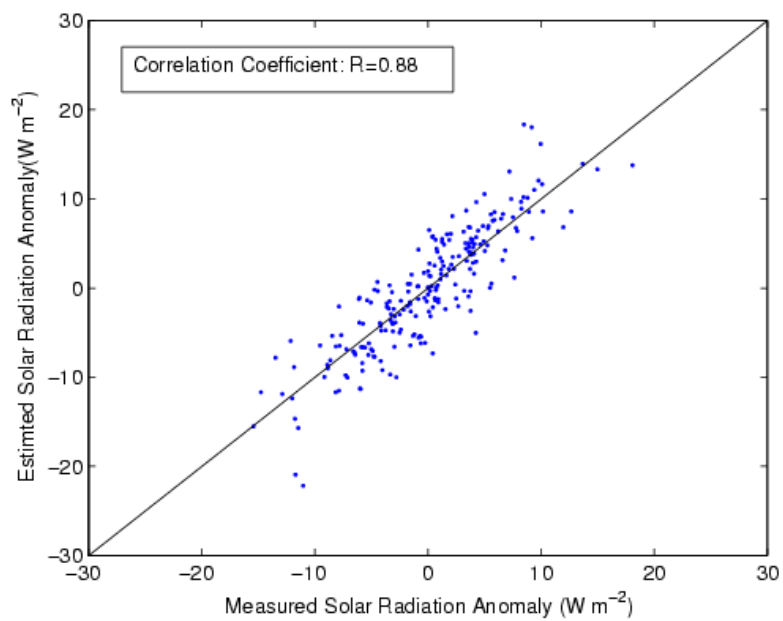


Fig. 5. Comparison between monthly regional R_s anomalies of measurements and our prediction from SunDu. The regional average is over 51 stations in China (Table 1). Each point represents one month.

14034

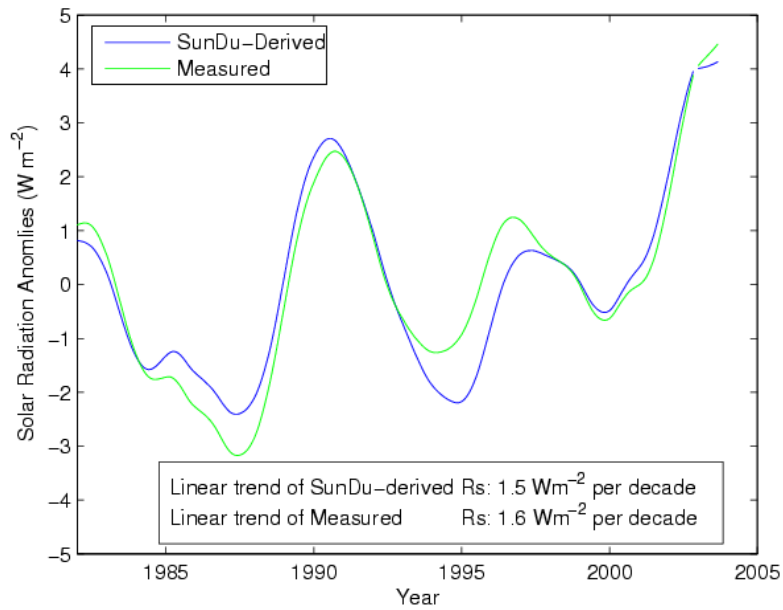


Fig. 6. Comparison of five-year smoothed monthly anomalies of SunDu-derived with directly-measured R_s averaged over 86 stations in Europe (Table 1). The breakpoint in 2003 reflects a break in data availability.

14035

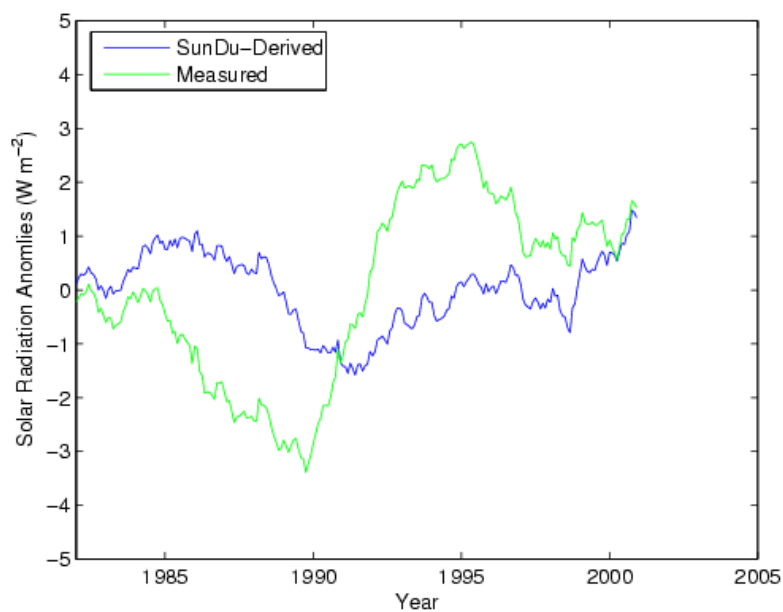


Fig. 7. Comparison of five-year smoothed monthly anomalies of SunDu-derived with directly-measured R_s averaged over 51 stations in China (Table 1). The sharp increase around 1991 in measured R_s occurred when Russian-made pyranometers (Type: DFY) were replaced by Chinese-made pyranometers (Type: TBS) from 1990 to the spring of 1993.

14036

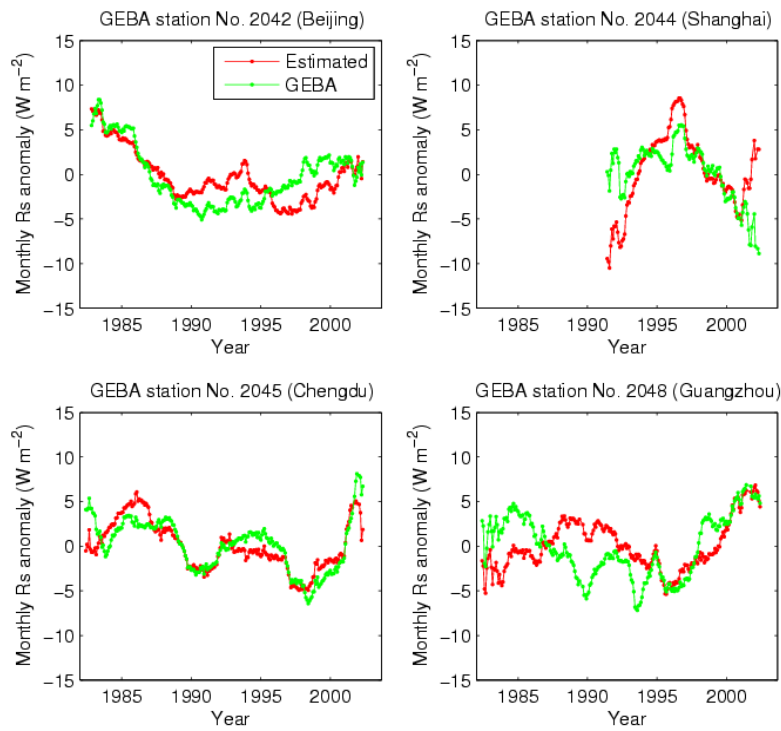


Fig. 8. Comparison between monthly SunDu derived and direct observed R_s at four baseline stations in China.

14037

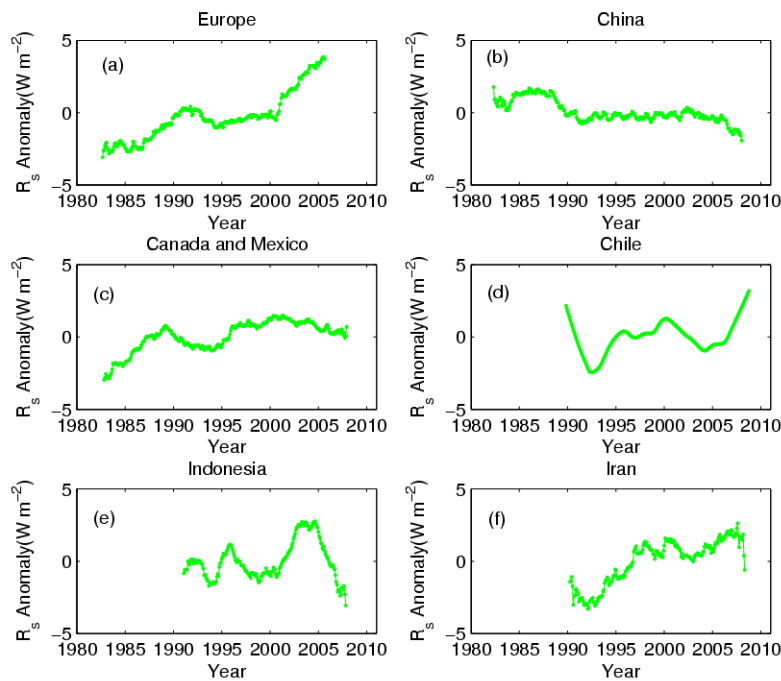


Fig. 9. Five-year smoothed monthly R_s anomalies derived from SunDu as averaged over geographic regions. The 1165 stations are divided into six regions based on the data availability and their trends: **(a)** Europe (35° N– 65° N, 10° W– 40° E), **(b)** China (20° N– 55° N, 55° E– 150° E), **(c)** North America (primarily Canada and Mexico, 15° N– 65° N, 160° W– 60° W), **(d)** Chile (60° S– 15° N, 90° W– 35° W), **(e)** Indonesia (20° S– 20° N, 65° E– 130° E), and **(f)** Iran (20° N– 50° N, 30° E– 55° E).

14038

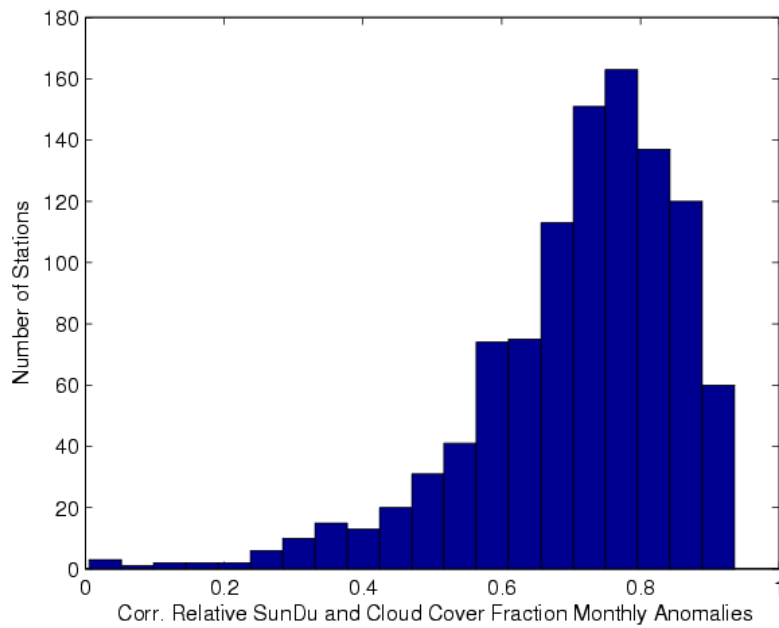


Fig. 10. Histogram of correlations between the relative SunDu (the ratio of measured SunDu to theoretical SunDu during a day) and monthly anomalies of total cloud cover fraction. Total cloud cover fraction is observed visually by trained technicians at weather stations. The plot shows that relative SunDu is highly correlated with cloud cover fraction on a monthly scale at most stations.

14039

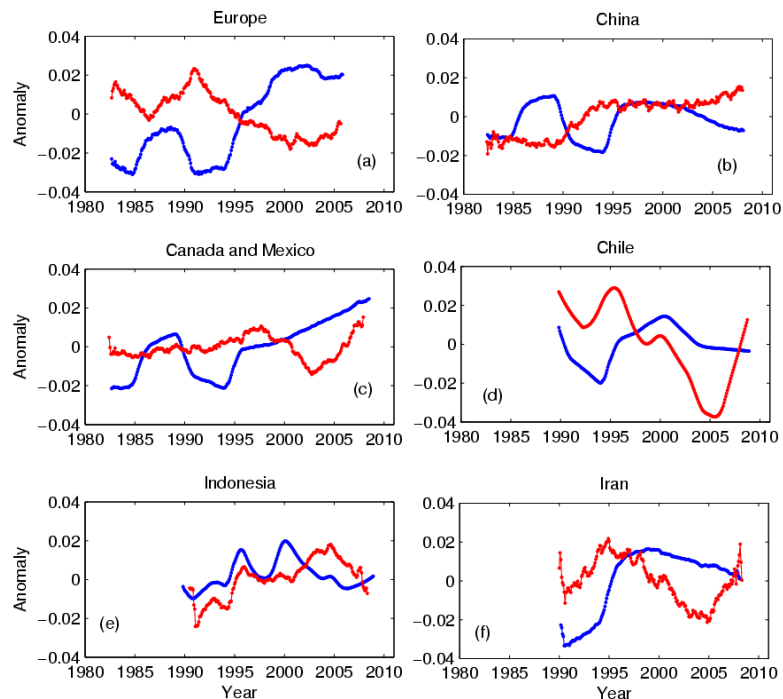


Fig. 11. Five-year smoothed clear-sky fraction derived from meteorological total cloud fraction measurement ($1 - F_c$, red Line) and negative of column aerosol optical depth ($-AOD$, blue Line). Clear sky fraction and negative AOD are shown here because they are positively correlated with R_s and can easily be compared with Fig. 9, i.e., both terms imply changes of R_s of the same sign.

14040

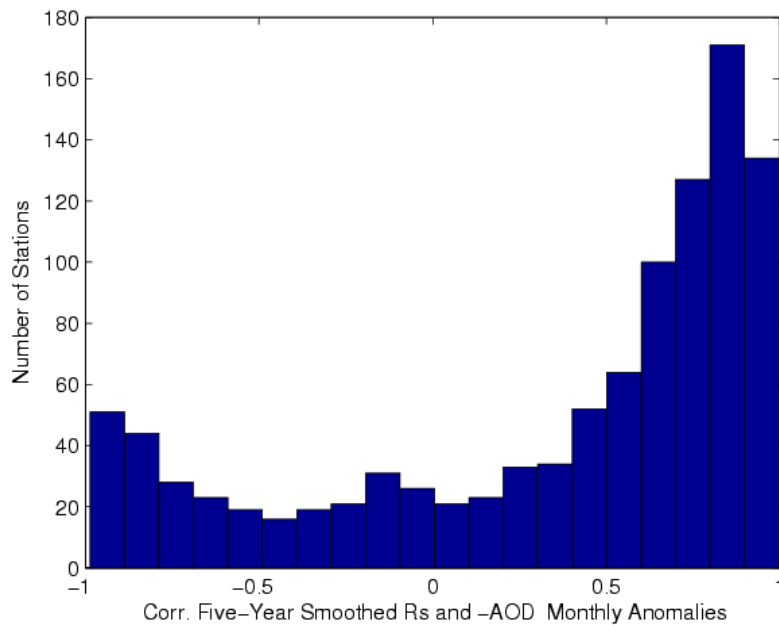


Fig. 12. The histogram of correlations between the five-year smoothed R_s and $-AOD$ monthly anomalies at each station. The five-year (60-month) smoothing filters out high frequency variations in R_s and $-AOD$ (shown in Figs. 9 and 11). About 58% of all stations have a correlation coefficient larger than 0.5. Such correlation coefficients indicate that the decadal variation in aerosols (Fig. 11) control the decadal variation in R_s (Fig. 9).

14041

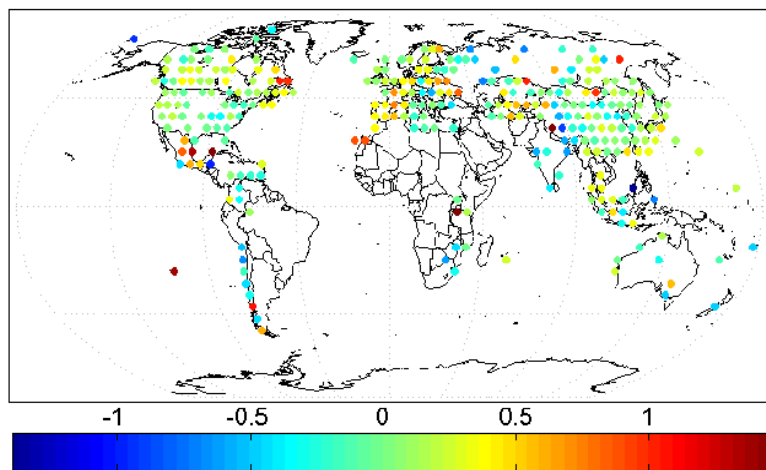


Fig. 13. The linear trend of R_s from 1982 to 2008 (unit: Wm^{-2} per year) by merging SunDu-derived values and direct measurements collected by GEBA. The trends are first calculated at each station and then aggregated into a $5^\circ \times 5^\circ$ grid and the averages are shown. There are 302 such grids obtained and shown.

14042